Theoretical Analysis of Steady State Low Current Arcs in Dual Flow Nozzles

K.D. Song*, Y.J. Shin, H.S. Lee, K.S. Kim
Korea Electrotechnology Research Institute

Abstract

When the circuit-breaker switches off, an electric arc is established between the contacts. It is very important to understand the arc characteristics for the design of a circuit breaker.

This article describes the theoretical analysis of the arc characteristics by means of energy integral method when convection dominated low current arcs are produced in the dual-airflow nozzle of a model interrupter. In order to investigate the arc radius, the average electric field strength and the arc voltage, the arc column is divided into two regions, and then the energy conservation equation is applied to the arc in each region together with the axial cold flow mass flux function, steady-state mass balance equation and Ohm's law. The results show good agreements with those of other researchers.

Introduction

Circuit breakers are required to control electrical power networks. They switch circuit on and off and carry the load under both normal and abnormal conditions by either a manual or an automatic operation.

When the circuit breaker switches off, the moving contact is drawn away from the fixed contact by an operating mechanism while gas begins to flow through the nozzle, thereby establishing an electric arc between the contacts. This arc is stabilized by the gas, which flows from a high-pressure reservoir through a nozzle to the exit.

It is very important to understand the arc characteristics for the design of a circuit breaker. Arc energy integral method has been utilized to analyze the arcs theoretically in a constant diameter nozzle flow[1], a 15° half-angle conical nozzle flow[2], an 8° half-angle conical nozzle flow[3], an orifice nozzle flow[4] and a dual nozzle flow[5].

In this research, the arc energy integral method is applied to quasi-stationary and convection dominated low current arcs in a dual airflow nozzle, considering the effects of shock waves which were neglected by a previous investigator[5]. In order to investigate the arc characteristics such as the arc radius, the electric field strength and the arc voltage, the arc established between contacts is divided into two regions, and then the energy conservation equation is applied together with an axial cold flow mass flux function, steady-state mass balance equation and Ohm's law to the control volume of a differential element of the arc in each region.

Arc Energy Integral Method

Assumptions

The arc and the cold flow can be represented by a two-zone channel model with a constant arc temperature and a constant velocity,as shown in Fig. 1.

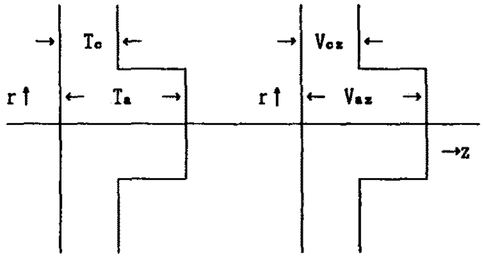

Fig. 1 Two-zone channel model

The arc energy integral method simplifies the analysis with the following assumptions.

(1) Local thermodynamic equilibrium is maintained.
(2) The flow is steady and axisymmetrical and the arc is cylindrical
(3) The radial pressure variation, $\partial P/\partial r$, is much smaller than the axial pressure variation, $\partial P/\partial z$, and therefore $\partial P/\partial r$ is neglected.
(4) The arc temperature is constant and independent on both radial and axial distance.
(5) Axial and radial heat conductions are negligible compared with heat convection.

Cold gas flow

Cold gas properties can be determined experimentally by pressure measurements or by a computational method[6]. The static pressures along the nozzle wall and the nozzle axis were measured for two different nozzle gap spacings[5].

These measured static pressure and the

reservoir pressure can be used to calculate the Mach number distribution along the nozzle axis, and then density, temperature, sonic velocity and axial velocity can be found from Mach number at each axial location with the following isentropic relations:

$$\frac{P}{P_o} = \left(1 + \frac{\gamma-1}{2}M^2\right)^{-\gamma/(\gamma-1)} \qquad (1)$$

$$\frac{\rho}{\rho_o} = \left(1 + \frac{\gamma-1}{2}M^2\right)^{-1/(\gamma-1)} \qquad (2)$$

$$\frac{T}{T_o} = \left(1 + \frac{\gamma-1}{2}M^2\right)^{-1} \qquad (3)$$

$$a = (\gamma RT)^{1/2} \qquad (4)$$

$$V_{cz} = Ma \qquad (5)$$

where P_o is the reservoir pressure, γ the specific heat ratio, ρ_o the reservoir air density, T_o the reservoir air temperature, R the gas constant, respectively. T_o is assumed to remain constant at room temperature, and the enthalpy can be calculated using the following equation:

$$h_c = C_p T \qquad (6)$$

where C_p is the specific heat at constant pressure. The static pressure distribution and the Mach number distribution functions are shown in Fig. 2.

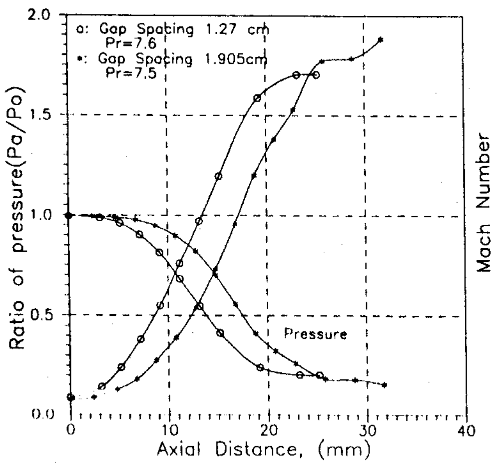

Fig. 2 Distributions of pressure and Mach number.

The continuous cold flow through the nozzle is assumed to be inviscid, uniform across the nozzle cross section and calorically perfect. The cold flow mass flux $\rho_c V_{cz}$ as a function of the axial distance in a dual flow nozzle is represented in Fig. 3 for 1.27 cm nozzle gap spacing and in Fig. 4 for 1.905 cm nozzle gap spacing with nozzle pressure ratios of 7.622 and 7.5.

It is reasonable to approximate the axial mass flux $\rho_c V_{cz}$ as piecewise linear functions of z for four regions:

$$\rho_c V_{cz} = a_n z + b_n, \quad z_n \le z \le z_{n+1} \quad n=1,2,3 \text{ and } 4 \qquad (7)$$

where z_1 corresponds to the stagnation point, z_2 a very small distance ε from the stagnation point, z_3 the nozzle throat, z_4 the shock wave location, and z_5 the nozzle exit. The a_n and b_n are constants and determined from the linear axial mass flux distribution functions.

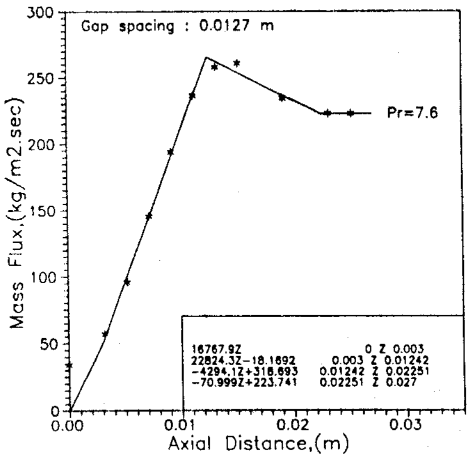

Fig. 3 Cold flow mass flux $\rho_c V_{cz}$ for a gap spacing of 1.27 cm.

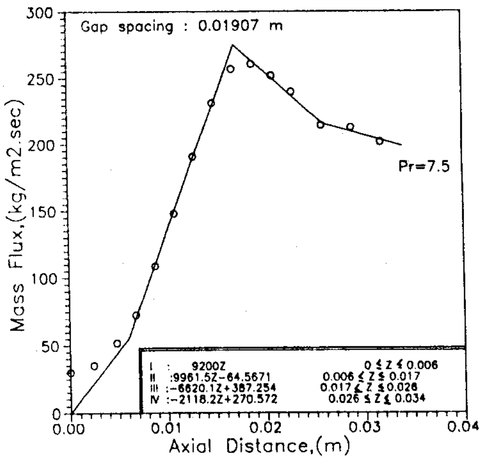

Fig. 4 Cold flow mass flux $\rho_c V_{cz}$ for a gap spacing of 1.905 cm.

Arc Plasma flow

The plasma flow in the arc is not adiabatic because of the ohmic heating, but is approximated by a constant temperature which is around 20000 °K. The momentum equation for the compressible, inviscid plasma flow is given by:

$$\rho_a V_{az} \frac{\partial V_{az}}{\partial z} = - \frac{\partial P_a}{\partial z} \qquad (8)$$

The plasma static pressure is assumed to be equal to the cold flow static pressure because the magnetic pinch pressure is negligible and the arc radius is small compared with the throat radius.

The plasma density can be expressed as:

$$\rho_a = \frac{P_a}{R\,T_a} \qquad (9)$$

Substituting this equation into Eq.(8) and integrating from the stagnation point to any axial location, the plasma velocity at that axial location is given by:

$$V_{az} = [\,2\,R\,T_a\,\ln(P_o/P_a)]^{1/2} \qquad (10)$$

From Eqs.(9) and (10), the plasma flow mass flux is given by:

$$\rho_a V_{az} = P_a\,[2\frac{\ln(P_o/P_a)}{R\,T_a}]^{1/2} \qquad (11)$$

Solution for Arc Characteristics

Since the cold flow mass flux and the plasma flow mass flux were determined by Eqs.(7) and (11), the conservation equations of mass and energy can be solved by considering the arc in the stagnation region.

1) Region I : $z_1 \le z \le z_2$

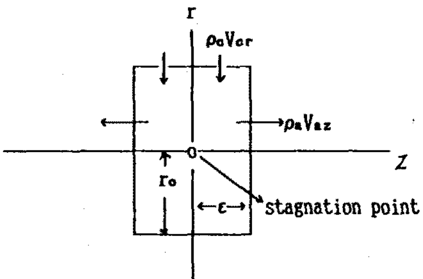

Fig. 5 A control volume of the differential element of an arc in region 1.

Applying the conservation of mass to the control volume of the differential element of an arc in Fig. 5, a steady-state mass balance equation yields:

$$2\pi r_o 2\varepsilon \rho_c V_{cr} = 2\pi r_o^2 \rho_a V_{az} \qquad (12)$$

where ε is a very small distance from the stagnation point. Applying the conservation equation of energy to the same control volume of the differential element of an arc, the steady-state energy balance equation yields:

$$\pi r_o^2 2\varepsilon(\sigma E^2 - U_t) = 2\pi r_o^2 \rho_a V_{az} h_a - 2\pi r_o \varepsilon \rho_c V_{cr} h_c \qquad (13)$$

where $(\sigma E^2 - U_t)$ is the net heat generation of the plasma due to the ohmic heating σE^2 and the radiation loss U_t, and h_a and h_c are the specific enthalpy of the arc plasma and the cold flow, respectively. The radiation loss U_t is negligibly small for a small current compared to the ohmic heating term σE^2. The kinetic energy is neglected because the radial and axial velocities are very small near the stagnation point.

Substituting Eq.(12) into Eq.(13) and then rearranging yields:

$$\sigma E^2 r_o = 2\rho_c V_{cr}(h_a - h_c) \qquad (14)$$

The simplified Ohm's law is

$$j = \sigma E \qquad (15)$$

where j is the current density. The electric field strength for a cylindrical arc is

$$E = \frac{I}{\pi r_o^2 \sigma} \qquad (16)$$

The axial cold flow mass flux $\rho_c V_{cz}$ can be approximated as a linear function of z with a constant $b_1=0$ as shown in Eq.(7) because the radial and axial velocities are obviously zero at the stagnation point, and it can be expressed as follows:

$$\rho_c V_{cz} = a_1 z \quad \text{for region 1} \qquad (17)$$

The radial cold flow mass flux $\rho_c V_{cr}$ can be determined by solving the following continuity equation.

$$\frac{1}{r}\frac{\partial}{\partial r}(r\rho_c V_{cr}) + \frac{\partial}{\partial z}(\rho_c V_{cz}) = 0 \qquad (18)$$

Substituting Eq.(17) into Eq.(18) and then integrating from the stagnation point to any radial position, the radial cold flow mass flux is given by:

$$\rho_c V_{cr} = -\,(a_1/2)r \qquad (19)$$

where the negative sign indicates inward flow direction into the differential control volume.

Substituting Eqs.(16) and (19) into Eq.(14), then the arc radius for region 1 is

$$r_{o1} = (\frac{I^2}{a_1 \pi^2 K_1})^{1/4} \qquad (20)$$

where the factor K_1 is given by:

$$K_1 = \sigma(h_a - h_c) \qquad (21)$$

The electric field strength for this region 1 can be obtained from Eqs.(16) and (20) and given by:

$$E_1 = (\frac{a_1 K_1}{\sigma^2})^{1/2} \qquad (22)$$

This region 1 is only applicable in the region near the stagnation point.

2) Region II : all the other regions

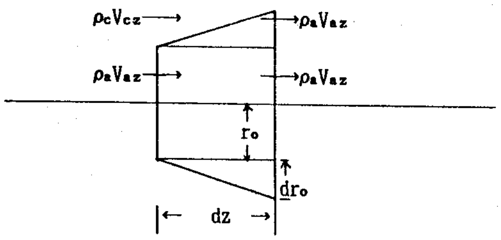

Fig. 6 A control volume of the differential element of an arc in region 2, 3 and 4.

Applying the conservation equation of mass to the control volume of the differential element of an arc in the region as shown in Fig. 6, a steady-state mass balance equation yields:

$$\rho_c V_{cz} 2\pi r_o dr_o + \rho_a V_{az} \pi r_o^2 = \rho_a V_{az} \pi r_o^2 + \frac{d}{dz}(\rho_a V_{az} \pi r_o^2)dz \qquad (23)$$

Applying the conservation equation of energy to the same control volume of the differential element of an arc, the steady-state energy balance yields:

$$\rho_a V_{az} \pi r_o^2 (h_a + \frac{1}{2} V_{az}^2) + \rho_c V_{cz} 2\pi r_o dr_o (h_a + \frac{1}{2} V_{cz}^2) + \sigma E^2 \pi r_o^2 dz = \rho_a V_{az} \pi r_o^2 (h_a + \frac{1}{2} V_{az}^2) + \frac{d}{dz}\{\rho_a V_{az} \pi r_o^2 (h_a + \frac{1}{2} V_{az}^2)\}dz \qquad (24)$$

Substituting Eq.(23) into Eq.(24) and rearranging gives the final energy balance in terms of the cold flow mass flux as:

$$\sigma E^2 \pi r_o^2 dz = \rho_c V_{cz} 2\pi r_o dr_o \{(h_a - h_c) + 0.5(V_{az}^2 - V_{cz}^2)\} \qquad (25)$$

The left-hand side is the heat generation of the plasma due to the ohmic heating in the differential control volume and the right-hand side is the energy absorbed to heat the cold gas flow to the arc temperature, and the kinetic energy to accelerate the cold flow to the arc velocity.

Substituting Eq.(16) into Eq.(25), then, the following equation can be obtained:

$$\frac{dz}{\rho_c V_{cz}} = \frac{\pi^2}{I^2} 2\sigma r_o^3 dr_o \{(h_a - h_c) + \frac{1}{2}(V_{az}^2 - V_{cz}^2)\} \qquad (26)$$

The linear piecewise approximation of Eq.(7) is substituted into Eq.(26) and then the differential equation is integrated in order to find the arc radius r_o for these regions by:

$$r_{on} = [\frac{4I^2}{\pi^2 K}\{\frac{1}{a_n}\ln(a_n z + b_n) + \phi_n\}]^{1/4}, \quad n=2,3 \text{ and } 4 \qquad (27)$$

where ϕ_n is the integration constant and K is given by:

$$K = \sigma\{2(h_a - h_c) + (V_{az}^2 - V_{cz}^2)\} \qquad (28)$$

The electric field strength for these regions can be obtained from Eqs.(16) and (27) as a function of the axial distance z by:

$$E_n = [\frac{K a_n}{4\sigma^2\{\ln(a_n z + b_n) + \phi_n a_n\}}]^{1/2}, \quad n=2,3 \text{ and } 4 \qquad (29)$$

The integration constant ϕ_n can be determined from the following condition that the arc radius is continuous along the nozzle axis:

$$r_{o1} = r_{o2} \text{ at } z = z_2, \quad r_{o2} = r_{o3} \text{ at } z = z_3, \quad r_{o3} = r_{o4} \text{ at } z = z_4 \qquad (30)$$

Applying these conditions to the arc radius equations, the integration constants are given by:

$$\phi_2 = K/(4K_1 a_1) - \ln(a_2 z_2 + b_2)/a_2 \qquad (31)$$

$$\phi_3 = \ln(a_2 z_3 + b_2)/a_2 + \phi_2 - \ln(a_3 z_3 + b_3)/a_3 \qquad (32)$$

$$\phi_4 = \ln(a_3 z_4 + b_3)/a_3 + \phi_3 - \ln(a_4 z_4 + b_4)/a_4 \qquad (33)$$

The arc voltage can be obtained by integrating the electric field strength over the total axial distances and is given for the pressure ratios by:

$$V_{arc} = 2(\int_{z_1}^{z_2} E_1(z)dz + \int_{z_2}^{z_3} E_2(z)dz + \int_{z_3}^{z_4} E_3(z)dz + \int_{z_4}^{z_5} E_4(z)dz) \qquad (34)$$

Results and Discussion

In this research, the arc radius, the electric field strength and the arc voltage with respect to the axial distance have been investigated for steady-state air arcs in a dual flow nozzle with upstream pressure of 0.1 MPa (1 atm), and a current in the range of 60 to 230 Amperes.

Fig. 7 shows the arc radius variation along the nozzle axis with the gap spacing of 1.27 cm. The radius increases linearly from 0.41 to 0.80 mm near the stagnation point, from 0.61 to 1.19 mm at the nozzle exit as the arc current increases from 60 to 230 Amperes. The arc radius variation along the nozzle axis with the gap spacing of 1.905 cm is shown in Fig. 8. The arc radius increases linearly from 0.48 to 0.93 mm near the stagnation point, from 0.73 to 1.43 mm at the exit as the arc current increases from 60 to 230 Amperes. The arc radius for the gap spacing of 1.905 cm increases more rapidly than that for the gap spacing of 1.27 cm at the downstream region, but the increase becomes slow suddenly at the axial distance of 0.026 m where the shock waves seem to occur.

Fig. 9 shows the average electric field strength variation as a function of the axial distance. The maximum electric field strength occurs near the nozzle throat, that has been found in the case of a single flow nozzle[7,8,9,10]. The average electric field strength is almost constant at the upstream region although the peak occurs near the nozzle throat, but decreases drastically at the downstream region. The average electric field strength remains almost constant albeit the arc current increases from 60 to 230 Amperes, which is typical in the medium current ranges of tens to hundreds Amperes. The values of the average electric field strength are 12.6 and 9.4 kV/m near the stagnation point, 13.0 and 9.7 kV/m near the nozzle throat, and 6.9 and 4.8 kV/m at the nozzle exit with the gap spacings of 1.27 cm and 1.905 cm, respectively.

Fig. 10 shows the arc voltage variation with respect to the axial distance at two different gap spacings. The arc voltage increases almost linearly as the axial distance increases. The arc voltage is approximately 1200 V at the gap spacing of 1.27 cm and 540 V at the gap spacing of 1.905 cm, which is very similar to the result of other research[11].

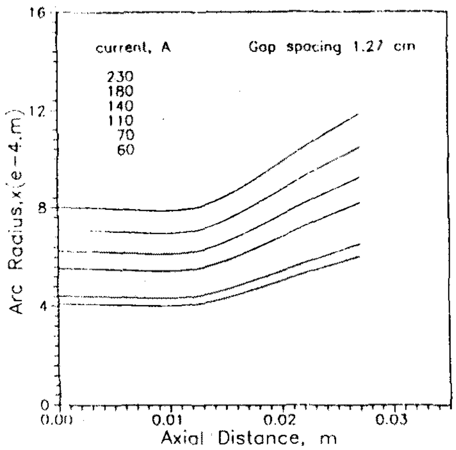

Fig. 7 Arc radius for a gap spacing of 1.27 cm.

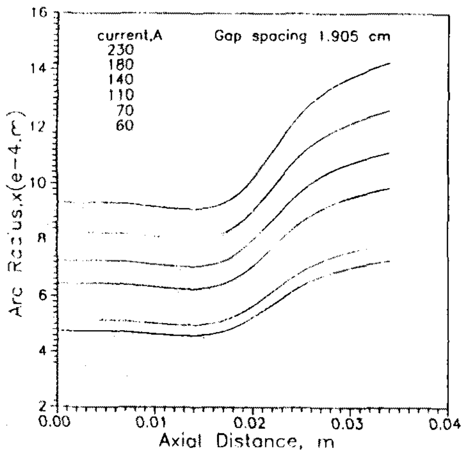

Fig. 8 Arc radius for a gap spacing of 1.905 cm.

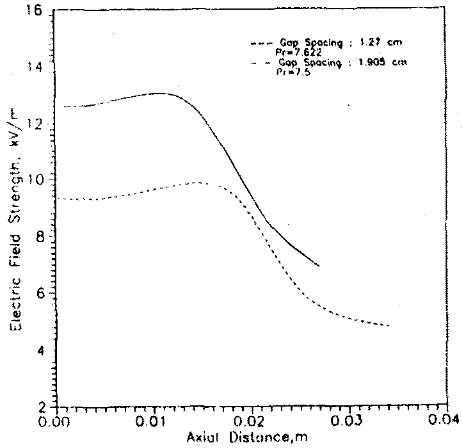

Fig. 9 Electric field strength for gap spacings of 1.27 and 1.905 cm

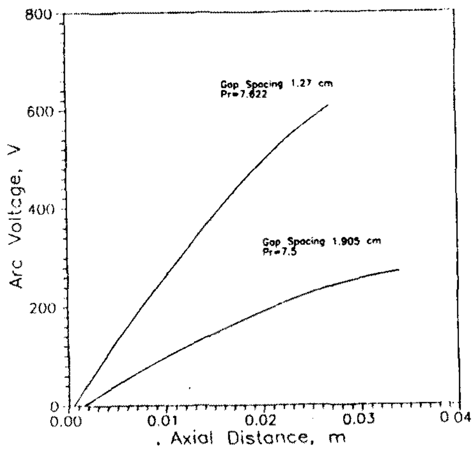

Fig.10 Arc voltage for gap spacing of 1.27 and 1.905 cm

Conclusions

In order to understand the characteristics of an arc produced in a dual-airflow nozzle, the arc radius, the average electric field and the arc voltage have been investigated with an upstream reservoir pressure of 0.1 MPa(1 atm) and a current range of 60 to 230 Amperes. The following conclusions can be drawn from this reseach:

1) The hot arc core is constricted at the upstream region, especially near the nozzle throat.

2) *In a dual-airflow nozzle, it may be the nozzle* throat which is the region critical to thermal capability in a circuit breaker, as is the case with a single flow nozzle.

3) The energy integral method can be an engineering means for the simplified design of a gas circuit breaker, as a matter of convenience.

References

1. H.T.Nagamatsu," Experimental and theoretical study of a d.c. arc in a constant diameter nozzle flow,"IEEE Paper No.81 SM468-8,July 1981.
2. H.T.Nagamatsu & P.G.Scavallo," An experimental and theoretical study of a d.c. arc in a 30° conical nozzle flow,"AIAA 18th Aerospace Sciences Meeting,Paper No.AIAA-80-0092, 1980.
3. H.T.Nagamatsu & P.D.Symolon," Experimental and theoretical study of a d.c. arc in a 8° conical nozzle flow,"AIAA 19th Aerospace Sciences Meeting,Paper No.AIAA-81-0097, 1981.
4. H.C.Whang & H.T.Nagamatsu," Experimental and theoretical study of a direct-current arc in an orifice nozzle flow,"AIAA Journal,Vol.23,No.7,July 1985.
5. I.Serbetci," Determination of the nature of steady and ramped convection stabilized air arcs near current zero,"Ph.D.Thesis,RPI,1989.
6. H.C.Whang," Experimental and theoretical results for low current d.c. arc in nozzle flows and calculations of cold flow field and correlations with experimental data for asymmetrical flow circuit breaker nozzles,"Ph.D.Dissertation,Rensselaer Polytechnic Institute,1986.
7. W.Hermann,U.Kogelschatz,L.Niemeyer,K.Ragaller & E.Schade," Experimental and theoretical study of a stationary high-current arc in a supersonic nozzle flow,"J.Phys.D:Appl.Phys.,Vol.7,1974,pp 1703 - 1721
8. W.Hermann,U.Kogelschatz,L.Niemeyer,K.Ragaller & E.Schade," Investigation on the physical phenomena around current zero in HV gas blast breakers,"IEEE Trans.PAS,Vol.PAS-95,No.4,1976,pp1165 - 1176
9. D.T.Tuma and J.J.Lowke," Prediction of properties of arcs stabilized by forced convection, "J.Appl.Phys., Vol.46,No.8,Aug.1975,pp3361 - 3367.
10. F.R.El-Akkari and D.T.Tuma," Simulation of transient and zero current behavior of arcs stabilized by forced convection," IEEE Trans. on PAS,Vol.PAS-96,No.6,Nov./Dec.1977,pp1784 - 1788.
11. S.Ramakrishnan,A.D.Strokes and J.J.Lowke,"An approximate model for high-current free-buring arcs," J.Phys.D:Appl.Phys.,Vol.11,1978,pp2267 - 2280